Traveling Wave Thermoacoustic Engine in a Looped Tube

T. Yazaki,[1,*] A. Iwata,[1] T. Maekawa,[1] and A. Tominaga[2]
[1]*Department of Natural Science, Aichi University of Education, Kariya 448, Japan*
[2]*Institute of Physics, University of Tsukuba, Tsujuba 305, Japan*
(Received 29 December 1997)

We have built a thermoacoustic engine consisting of a differentially heated stack of plates in a looped tube and observed spontaneous gas oscillations of the traveling wave mode running around the loop. Stability boundary and thermally produced acoustic power are compared with those for the engine tested in a resonator. The engine in a looped tube acts as a traveling wave power amplifier, whose onset temperature ratios are significantly smaller than those for the engine in a resonator. [S0031-9007(98)07330-X]

PACS numbers: 43.35.+d

Thermal interactions between solid walls and oscillating gas produce a rich variety of thermoacoustic phenomena such as self-sustained gas oscillations and acoustic heat pumping [1–3]. Wheatley and his group [4] have reexamined the phenomena from the standpoint of thermodynamics, developing Rayleigh's idea of heat engine [5], and proposing important quantities of heat flow Q and work flow I as basic concepts in thermoacoustics [6]. The work source $W(\equiv \nabla I)$ [3,6] is equivalent to the acoustic power per unit volume produced by the energy conversion of Q to I. The energy conversion between Q and I occurs in a *stack of plates*, resulting in the two classes of engines. One is the *prime mover* (spontaneous oscillations) converting Q to I ($W > 0$), and the other is the heat pump converting I to Q ($W < 0$). These ideas of thermoacoustic engines [1,4] may be applied to general engines having a *regenerator* such as Stirling engines [7] and pulse tube refrigerators [8]. Understanding such heat engines is one of the fundamental problems in thermoacoustics.

Much of the recent experimental work [9] in thermoacoustics has concentrated on the standing wave engine in an acoustic resonator. However, Ceperley [10] proposed a *looped tube* with a differentially heated regenerator as the traveling wave heat engine with no piston or any other moving parts. We have now designed, built, and tested a thermoacoustic engine consisting of a stack and two heat exchangers in a looped tube and observed spontaneous gas oscillations of the traveling wave mode running around the loop and through the stack from cold to hot. This device functions as a traveling wave engine. In this Letter we report measurements of the stability boundary between oscillatory and nonoscillatory regions and thermally produced acoustic power for the traveling wave engine and compare the results with those for the standing wave engine tested in a resonator.

Thermoacoustic energy conversion is essentially controlled by two parameters. One is $\omega\tau$, where ω is the angular frequency of gas oscillation, and τ is the time required for thermal equilibrium in the cross section of the flow channel. The time τ is given by $r^2/2\alpha$, where r is the characteristic transverse length of the channel, and $\alpha = \kappa/c_p\rho_m$ is the thermal diffusivity of gas; κ, c_p, and ρ_m are thermal conductivity, isobaric heat capacity per unit mass, and mean density, respectively. If $\omega\tau \ll 1$, the gas in the channel moves reversibly, equilibrating at the local wall temperature, whereas if $\omega\tau \gg 1$, the gas motion becomes isentropic but still reversible to a good approximation. However, the oscillating gas becomes thermodynamically irreversible near $\omega\tau \sim 1$ due to incomplete heat transfer to the wall.

The second controlling parameter is the phase delay between pressure $P = pe^{i\omega t}$ and cross-sectional mean velocity $V_m = \nu_m e^{i(\omega t+\Phi)} = \nu_m \sin\Phi\, e^{i(\omega t+\pi/2)} + \nu_m \times \cos\Phi\, e^{i\omega t}$. We call $\nu_m \sin\Phi$ the *standing wave component* (SWC) of V_m, which is $\pi/2$ out of phase with P, and $\nu_m \cos\Phi$ the *traveling wave component* (TWC), which is in phase with P. Only the TWC contributes to I, and the acoustic energy travels in the same direction as the wave.

A schematic diagram of our experimental setup is shown in Fig. 1. The cavity consists of a looped stainless steel tube of inner radius 20.1 mm and average length $L = 2.58$ m, replaced in part by a glass cylinder with inner radius $r_0 = 18.5$ mm for velocity measurements by laser Doppler velocimetry (LDV). The tube is filled with air as a working gas and contains a stack and two heat exchangers. Hot and cold heat exchangers are attached to both sides of the stack with side wall temperatures of T_H and T_C; most of the tube body, as well as T_C, is at room temperature. The 40 mm long stack is made of a ceramic catalyst containing many square channels with cross section $2r \times 2r$ ($r = 0.44$ mm). The pressure at 24 places around the loop was simultaneously measured by small sensors mounted on the walls and digitized by fast 12-bit analog-to-digital (A/D) converters. The spatiotemporal evolution of the acoustic pressure P, which was obtained by reconstructing the 24 signals, was used to identify the wavelength λ and the direction of wave propagation.

Spontaneous gas oscillation takes place when the hot temperature T_H exceeds a threshold value which is dependent on the mean gas pressure P_m. The frequency

 0031-9007/98/81(15)/3128(4)$15.00

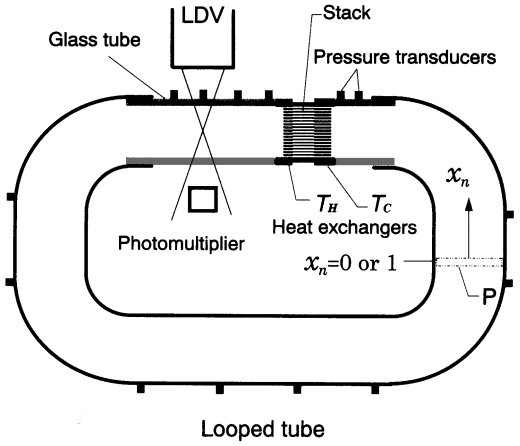

FIG. 1. Schematic experimental device equipped with a thermoacoustic engine consisting of a stack and two heat exchangers. T_H and T_C are the temperatures of the hot and cold heat exchangers attached to the stack. Small pressure sensors are mounted on the wall at 24 places around the loop. For the looped tube, the partition (P) is not equipped. For the *resonance tube*, the tube was completely blocked by a partition. The optimum position of the partition where the thermoacoustic effect is the most effective for the standing wave with $\lambda = L/2$ (L is the total length of the loop) is defined as $x_n = 0$, where x_n is the coordinate around the loop normalized by L. Then the center of the stack is at $x_n = 0.19$.

$f = \omega/2\pi$ was 268 Hz at atmospheric pressure. From the spatiotemporal evolution of P, we found that the oscillation is of the acoustic traveling wave mode with $\lambda = L/2$ (the second mode) running around the loop through the stack from cold to hot. Therefore, a stack and two heat exchangers in the looped tube acts as a traveling wave engine.

To map out the stability boundary between oscillatory and nonoscillatory regions, we used the dimensionless numbers T_H/T_C and $\omega\tau$ at the mean temperature $(T_H + T_C)/2$ in the stack [2]. The boundary was explored by gradually changing τ through the mean pressure P_m at a constant ratio T_H/T_C; increasing P_m increases the mean density ρ_m, thereby decreasing α and increasing τ. Figure 2 shows a log-log plot of the onset temperature ratio vs $\omega\tau$, where ω obtained in small amplitude region was adopted for determining the critical value of $\omega\tau$ [11]. The data for the looped tube are shown by the open circles. The frequency f ($\simeq$ 268 Hz) of the second mode changes by only 1.5% over the whole stability curve.

Next the looped tube was completely blocked by a partition, as shown in Fig. 1, which is thin, flat, and rigid so that it does not change the length of the loop. We searched for spontaneous gas oscillations of the standing wave mode with the same wavelength ($\lambda = L/2$) and frequency ($\simeq$268 Hz) as the traveling wave mode by adjusting the position of the partition along the loop. The oscillations were observed to be of the standing wave mode from the spatiotemporal evolution of P. We measured onset temperature ratios at atmospheric pressure for various positions of the partition and fixed the partition at the optimum position where the thermoacoustic effect is maximum (with minimum onset temperature ratio). We call this tube a *resonance tube* (or a *resonator*). The final position of the partition was denoted as $x_n = 0$ (see Fig. 1), where x_n is the axial coordinate normalized by L. Then the center of the stack was at $x_n = 0.19$, which is approximately $\frac{3}{16}$, the midpoint between pressure node and velocity node of a nondissipative standing wave with $\lambda = L/2$ in a resonator. The experimental data for the resonance tube are shown by the solid circles in Fig. 2, indicating the standing wave stability curve.

The oscillation is produced in a limited range of $\omega\tau$ above a threshold temperature ratio, and there are two stability limits corresponding to the right- and left-hand branches. Such standing wave stability curves have already been studied theoretically [12] and experimentally [9]. According to Wheatley *et al.* [4], the existence of the two limits for the resonance tube implies that the thermodynamical process of the working gas in the stack is intrinsically irreversible for the standing wave mode. The right branches for the resonance and looped tubes are due to lack of heat exchange between the gas and stack walls, so the two asymptotic stability lines for $\omega\tau \gg 1$ are effectively identical.

These experimental stability curves show that the traveling wave thermoacoustic engine has smaller onset temperature ratios at all values of $\omega\tau$ measured, which spans the range 0.5 to 5.0, compared with those for the standing wave engine which relies on an irreversible process to operate. The remarkable reduction (about 25% at $\omega\tau \sim 2$) of the critical temperature ratio is important for the application of thermoacoustic engines.

The most significant difference in the stability curve occurs along the left branch. A big reduction (about 70% at $T_H/T_C \sim 3$) of the critical relaxation time τ was observed for the looped tube compared with the standing wave stability curve. Such a significant depression of the left branch toward the left ($\omega\tau \ll 1$) suggests that

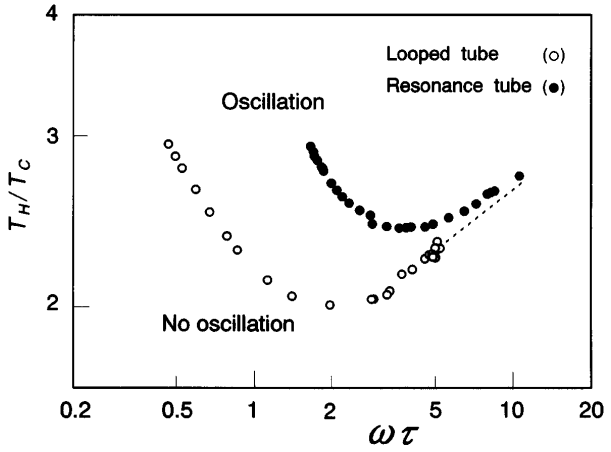

FIG. 2. A log-log plot of onset temperature ratio T_H/T_C vs $\omega\tau$, showing the boundary between oscillatory and nonoscillatory regions. The open and solid circles are for a traveling wave in a looped tube and a standing wave in a resonance tube, respectively.

excellent thermal contact between the gas and stack walls is favorable to the looped tube engine, whereas imperfect thermal contact is favorable to the standing wave engine. The stack in the looped tube performs the same functions as the regenerator in the Ceperley's reversible engine which needs a locally isothermal process ($\omega\tau \ll 1$) to operate. The left limit, however, for the tube is attributed to strong damping by viscous energy losses in the stack and heat exchangers, where a viscous boundary layer of thickness $\delta = (2\mu/\rho_m\omega)^{1/2}$ (μ is the dynamic viscosity of gas) fills up the channel with decreasing $\omega\tau$. Spontaneous oscillation, therefore, might be observed at $\omega\tau \ll 1$, if the viscous energy losses are sufficiently small.

We took velocity measurements near the center of the tube by LDV through a glass section of the loop in order to determine the work flow $I = \overline{PV_m}$ (the bar indicates the time average, and V_m is the cross-sectional mean velocity given by $\nu_m e^{i(\omega t+\Phi)}$). Pressure $P = pe^{i\omega t}$ (independent of the radial coordinate) and axial velocity near the center $V_c = \nu_c e^{i(\omega t+\psi_c)}$ at a given position of x_n were simultaneously digitized, and their power and phase spectra were calculated via fast Fourier transform from the time series of 16 384 points.

The oscillating flow was laminar everywhere, and their power spectra consisted of sharp peaks at f and its harmonics nf. The amplitudes $p(nf)$ and $\nu_c(nf)$ of P and V_c were determined from the power spectra. The phase lead $\psi_c(nf)$ of V_c was also obtained from the phase spectra and corrected for delays caused by the experimental systems. We estimated the amplitude and phase $\nu_m(nf)$ and $\Phi(nf)$ of the mean velocity from measured $\nu_c(nf)$ and $\psi_c(nf)$ using the theoretical solutions of a laminar oscillating flow, namely, $\nu_m(nf) = \Gamma^{-1}(nf)\nu_c(nf)$, and $\Phi(nf) = \psi_c(nf) + \psi_o(nf)$. Both Γ and ψ_0 depend on the parameter r_0/δ in the glass cylinder (r_0 is the inner radius of the glass cylinder). Thus, the experimental work flow was determined from

$$I = \frac{1}{2}\sum_{n=1} p(nf)\nu_c(nf)\Gamma^{-1}(nf) \times \cos\{\psi_c(nf) + \psi_o(nf)\},$$

where the laminar theory gives $\Gamma(f) = 1.007$ and $\psi_o(f) = 0.42°$ for our case of $r_0/\delta \simeq 1.4 \times 10^2$. The factor ψ_o has substantial influence on the standing wave work flow because $\psi_c(f)$ is close to 90°.

Measurements of the work flow were performed in the oscillatory regions of the stability curves for the looped and resonance tubes at atmospheric pressure. The average pressure amplitude $p_a(f)$ was kept at about 0.82 kPa by adjusting T_H. Then the axial average of $\nu_c(f)$ within a glass cylinder was about 2.8 m/s. The two tubes are nearly equal in the energy losses by the viscous and thermal attenuation of sound except at the stack and heat exchangers.

The experimental phase variation $\Phi(x_n)$ for $n = 1$ is shown in Fig. 3(A). Real thermoacoustic engines have waves that are neither pure traveling wave ($\Phi = 0$) nor standing wave ($\Phi = \pi/2$) but are composed of both components. The looped tube ($T_H = 640$ K and $\omega\tau \simeq 3.3$ at the stack) is dominated by TWC, while the resonance tube ($T_H = 755$ K and $\omega\tau \simeq 2.7$) has mostly SWC except near the minima of p and ν_c. The spatial phase distribution is stationary; the phase at the looped tube stack interpolated from the outside was always about 25°, while the phase at the resonance tube stack was close to 90°.

Although traditional heat engines are made to operate at an optimum point in a thermodynamical cycle using moving parts such as pistons and valves, the traveling wave thermoacoustic engine performs an efficient thermodynamic cycle at a given value of $\omega\tau$ by tuning Φ to the optimum phase (about 25° at $\omega\tau \simeq 3.3$) without using any moving parts. Both TWC and SWC contribute to energy conversion from Q to I [3], and TWC and SWC contribute through reversible and irreversible thermodynamical processes, respectively [10]. Therefore, the addition of a small SWC to a traveling wave improves engine efficiency by correcting for a finite time delay τ in the stack. Another effect of a small amount of SWC added to a traveling wave is to reduce the viscous energy losses in the stack by reducing the velocity amplitude in the stack. Pure traveling wave energy conversion might be realized in a reversible process ($\omega\tau \ll 1$) for a working fluid but only with zero viscosity to achieve the ideal Stirling thermodynamic cycle [7].

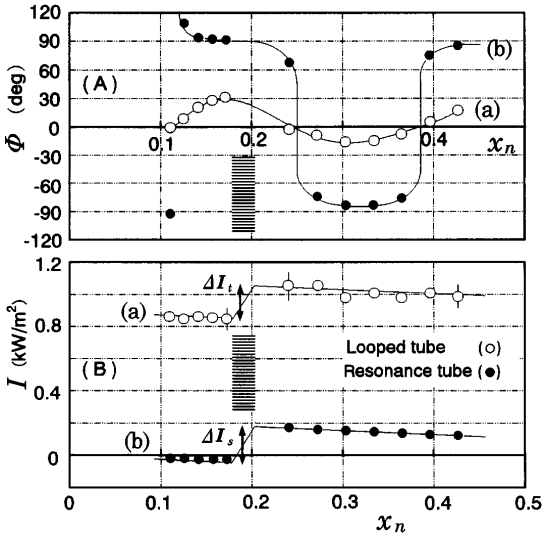

FIG. 3. (A) The phase distribution $\Phi(x_n)$ for (a) the looped tube and (b) the resonance tube. The lines are guides to the eye. The shaded region shows the location of the thermoacoustic engine. (B) Corresponding work flow. For (b), the lines to the right and to the left of the stack are linear fits with the same slope and drawn in such a way that $I(x_n = 0) = I(1) = 0$, resulting in the jump ΔI_s indicating the power produced by the stack. For (a), the lines are linear fits with the same slope as (b) and drawn in such a way that $I(x_n = 0) = I(1)$. The produced power ΔI_t of about 200 W/m^2 is nearly equal to ΔI_s.

The measured work flow is shown in Fig. 3(B), where the flow direction is to the right (from cold to hot) or the left according to whether I is positive or negative, respectively. The higher harmonics ($n = 2, 3 \ldots,$) of I are negligibly small (less than 2%) compared with the fundamental ($n = 1$). In the looped tube, the acoustic power (per unit area) of the traveling wave propagating from cold to hot increases by ΔI_t (more than 200 $\mathrm{W/m^2}$) indicated by the difference in I between the two sides of the stack, whenever the wave passes through the differentially heated stack. In other words, the looped tube engine acts as a traveling wave power amplifier whose gain (defined as the ratio of the output work flow to the input at the stack) is about 1.2 for $p_a(f) \simeq 0.82$ kPa. The produced power ΔI_t compensates for the dissipation of acoustic power at the tube walls, since the oscillation is sustained at constant amplitude p_a. Consequently, the acoustic power decreases linearly along the tube with $I(x_n = 0) = I(1)$ as shown in Fig. 3(B).

Although the power produced in the two configurations, ΔI_s and ΔI_t, is nearly equal, it flows out of the stack to the right and left and decreases to zero at the ends ($x_n = 0$ and 1) in the resonance tube to compensate for the energy losses. The stack acts as a source of acoustic power for the standing wave. Both the looped tube and the resonance tube have a positive work source of at least $W = \Delta I/\Delta x \sim 5\ \mathrm{kW/m^3}$ at the stack and negative work sources of about $-80\ \mathrm{W/m^3}$ in all other regions due to surface attenuation.

Ceperley [10] and several other authors [1,3,13] proposed that Stirling engines and related devices such as pulse tube refrigerators with a regenerator may be understood from the viewpoint of traveling wave thermoacoustic systems. Our results seem to confirm this insight; the time phasing between P and V_m in our traveling wave engine is substantially the same as in the regenerator of the Stirling engine. There is, however, a significant difference between Stirling and traveling wave thermoacoustic engines in that $\nu_m/a \ll p/P_m$ (a is adiabatic sound speed and p is pressure amplitude) in the regenerator ($\nu_m/a \sim 10^{-2} p/P_m$ for real Stirling engines), while $\nu_m/a \sim p/P_m$ in the stack for our case. Stirling engines, therefore, can operate at $\omega\tau \simeq 10^{-2}$, overcoming small viscous energy loss in a regenerator, in contrast with the traveling wave stability curve shown in Fig. 2. Because it does not need moving parts, the looped tube is potentially a powerful tool for applications such as traveling wave power amplifiers and Stirling engines and refrigerators. To realize such applications, we would propose something like a tuning column of a liquid Stirling engine [14] to satisfy the condition $\nu_m/a \ll p/P_m$.

In summary, we have tested a thermoacoustic engine in a looped tube and observed spontaneous gas oscillations running around the loop through the engine from cold to hot as a traveling wave. The looped tube engine is an energy conversion device generating acoustic power. The acoustic traveling wave is amplified by the power produced. Both TWC and SWC contribute to energy conversion performed in the thermoacoustic engine. The traveling wave engine which intrinsically needs excellent heat exchange between a working gas and stack walls has significantly smaller onset temperature ratios compared with the standing wave engine which relies on an irreversible process to operate.

*Electronic address: tyazaki@auecc.aichi-edu.ac.jp; Fax No.: 0566-26-2634.

[1] G. W. Swift, Phys. Today **48**, No. 7, 22 (1995); J. Acoust. Soc. Am. **84**, 1145 (1988).

[2] T. Yazaki, S. Takashima, and F. Mizutani, Phys. Rev. Lett. **58**, 1108 (1987); T. Yazaki, S. Sugioka, F. Mizutani, and H. Mamada, Phys. Rev. Lett. **64**, 2515 (1990); T. Yazaki, Phys. Rev. E **48**, 1806 (1993).

[3] A. Tominaga, Cryogenics **35**, 427 (1995); in *Proceedings of ASA/ASJ 3rd Joint Meeting, Honolulu, 1996* (Acoustical Society of Japan, Tokyo, 1996), p. 611.

[4] J. C. Wheatley, T. Hofler, G. W. Swift, and A. Migliori, Phys. Rev. Lett. **50**, 499 (1983); J. Acoust. Soc. Am. **74**, 153 (1983); Am. J. Phys. **53**, 147 (1985).

[5] Lord Rayleigh, in *The Theory of Sound* (Dover, New York, 1945), Sec. 322f-i.

[6] Heat flow Q and work flow I are defined as $Q = \rho_m T_m \langle SV \rangle$ and $I = \overline{\langle PV \rangle}$, where angular brackets indicate radial average; ρ_m, T_m, S, and V are mean mass density, mean temperature, entropy per unit mass, and axial velocity, respectively. The work flow is equivalent to the acoustical intensity defined in acoustics. The thermodynamic equations produce the relation, $H = Q + I$, where H is the enthalpy flow. In constant cross-sectional regions without heat exchangers, $\nabla Q + \nabla I = 0$, which shows full energy conversion between Q and I. We call ∇I the work source W.

[7] I. Urieli and D. M. Berchowits, *Stirling Cycle Engine Analysis* (Hilger, Bristol, UK, 1984).

[8] W. E. Gifford and R. C. Longsworth, in *International Advances in Cryogenic Engineering* (Plenum, New York, 1966), Vol. 11, p. 171.

[9] A. A. Atchley, J. Acoust. Soc. Am. **95**, 1661 (1994); A. A. Atchley and F. Kuo, J. Acoust. Soc. Am. **95**, 1401 (1994); T. Yazaki, A. Tominaga, and Y. Narahara, J. Low Temp. Phys. **41**, 45 (1980); T. Yazaki and A. Tominaga, Proc. R. Soc. London A **454**, 2113 (1998).

[10] P. H. Ceperley, J. Acoust. Soc. Am. **66**, 1508 (1979).

[11] Further increase of P_m along the stability curve leads to the onset of the fundamental mode with $\lambda = L$ and $f \simeq 137$ Hz instead of the second mode. Stability curves for two different oscillatory modes can intersect each other which leads to complex phenomena such as mode competition and quasiperiodicity near the stability curve crossing.

[12] N. Rott, Z. Angew. Math. Phys. **20**, 230 (1969); Z. Angew. Math. Phys. **24**, 54 (1973).

[13] S. L. Garrett and G. W. Swift, in *Proceedings of the 7th International Conference on Stirling Cycle Machines, Tokyo, 1995* (The Japan Society of Mechanical Engineering, Tokyo, 1995), p. 23.

[14] C. D. West, *Liquid Piston Stirling Engines* (Van Nostrand Reinhold, New York, 1983).